A Dynamical Description of Alkali Metal Cyanides with Extended Three Body Force Shell Model

Shemim S S[1], Anshida Mayeen [2] FergyJohn[3], N K Gaur[4]

[1]*Department of Physics, TKM College of Engineering, Kollam, Kerala, India*
[2]*Inter University Centre for Nanomaterials and Devices (IUCND) CUSAT, Kochi, Kerala, India*
[3]*Department of Physics, St Gregorious College, Kottarakkara, Kollam, Kerala, India*
[4]*Director,UIT, Dept of Physics, Barkathullah University, Bhopal, M.P, India*

Abstract

The nature of binding forces of a crystal can be unraveled by investigating the mechanical properties of pure crystals which include their cohesive, thermal and elastic properties. The variation of these properties in Alkali cyanides such as NaCN, KCN and RbCN with temperature were computed by means of Extended Three Body Force Shell Model (ETSM). The potential model of ETSM integrates the effect of coupling of the translation and orientation modes of the molecules in a crystal in the frame work of Three Body Force Shell model. The second order elastic constants of the three pure alkali cyanides of NaCN, KCN and RbCN were computed using ETSM at a very low temperature range. This paper presents a study which indicates the elastic softening at very low temperatures. The calculation of thermodynamic and cohesive properties such as Restrahlen frequency (ϑ_0), molecular force constant (*f*), Debye temperature (θ_D), cohesive energy (Φ) and Gruneisen parameter (γ) at very low temperatures were carried out with the theory of ETSM. The present study reveals that the elastic constants are reduced by the translational - rotational coupling effect at the zone center and the computed results are found to be in closer agreement with experimentally observed data. The theoretical work presented in this paper shows that the potential model ETSM is successful in comprehending the effect of coupling between the translational and rotational modes in the cohesive, thermal and elastic properties of pure alkali cyanides at very low temperatures.

Keywords: ETSM; Elastic constants; Cohesive Properties; Thermal properties.

1. Introduction

The transition from solid to liquid phase for some organic materials exhibit a cascade of transitions involving multiple new phases instead of a single transition phase. Mechanical and symmetry properties of these phases are intermediate between liquid and crystal phases and they are termed as liquid crystals. The intermediate phases between crystal phases and liquid phases are partially ordered phases. The position and orientation of the molecules of a normal crystal are ordered and have some completely ordered ideal structure with minimum potential energy. Some deviations occur due to the thermal excitation of phonon vibrational modes. But in liquids, there is no translational or orientational order. These phases occur due to the shapes of the molecules and depends on the comparative strength of the anisotropic and isotropic terms of the intermolecular potential [1].The partially ordered phases constitutes liquid crystals with translational disorder and orientational order and also crystals with translational order and orientational disorder. The latter known as Orientationally Disordered Crystals [2] (ODM) are common in nature but are not well known as the former liquid crystals. Most of their properties are affected by translational-rotational coupling [3-8]. The most important examples for ODM's are Alkali cyanides which are complex molecular ionic crystals with a pseudo-cubic Rock salt or Cesium Chloride structure. In these materials there will be an orientational disorder with respect to head and tail of CN^- ions. The alkali cyanides have general composition $M^+(XY)^{-1}$ which shows peculiar collective phenomenon due to the interaction between the $(XY)^{-1}$ radicals [9]. In pure crystal like NaCl when an ion like CN^- replaces the Cl^- ions, an excess negative charge is introduced in it. This replacement gives rise to charge compensating point defects due to the ionic impurities. Further, depending on the ionic radius of the doped ion, the impurity ion can occupy substitutional or interstitial position. So the impurity ion will behave as the lattice ion if it replaces that particular ion and will contribute the same charge to the lattice ion. In certain crystals, the non-spherical cyanide ions can obtain spherical symmetry by rotation [4, 10].

The physical and the dynamical properties of solids are determined by the inter-atomic or inter-ionic interactions in the solids [11]. The long-range attractive forces in solids caused by electrostatic Coulomb attraction between the valence electrons and the ions overwhelm the short-range repulsive forces that arise when the inner closed shells of electrons in atoms come into

contact. An equilibrium inter-atomic separation exists at which the Columbian force and the repulsive interaction force balance each other and make the solid stable.

2. Methodology and Theory

The potential model of ETSM [12] was formulated considering the ionic interaction potentials as,

$$\Phi = \Phi_c + \Phi_{TBI} + \Phi_{vdW} + \Phi_{SR} + \Phi_{TR}$$

$$= \frac{-1}{2}\sum_{kk'} \frac{Z_k Z_{k'}}{|\acute{r}_{kk'}|} e^2 + \frac{-1}{2}\sum_{kk'k} \frac{Z_k Z_{k'}}{|\acute{r}_{kk'}|} e^2 f(r_{kk''}) - \sum_{kk'} c_{kk'} r_{kk'}^{-6} - \sum_{kk'} d_{kk'} r_{kk'}^{-8} +$$

$$\sum_{kk'} b\beta_{kk'} e^{\frac{r_k + r_{k'} - r_{kk'}}{\rho}} + \Phi_{TR} \quad (1)$$

The first term in equation (1) refers to the long-range coulomb interaction energy and the second term is the long-range three body interaction energy. The Van der Waals dipole-dipole and dipole-quadrapole interactions are expressed as the third and fourth terms where, $c_{kk'}$ and $d_{kk'}$ represents the corresponding Van der Waals coefficients respectively [6]. The short-range overlap repulsion explained by Hafemeister and Flygare [5] applied up to the second neighbour ions is given as the fifth term. Here, $\beta_{kk'}$is the Pauling coefficient, b is the hardness parameter and ρ is range parameter. Φ_{TR} is the contribution due to the coupling of translational and rotational modes which is expressed as the last term [13, 14]. The Pauling coefficient $\beta_{kk'}$is given as,

$$\beta_{kk'} = 1 + \frac{Z_k}{n_k} + \frac{Z_{k'}}{n_{k'}} \quad (2)$$

where, n_k *and* $n_{k'}$ are the number of electrons in the outermost orbit of the ions and Z_k *and* $Z_{k'}$ are the valencies of the ions.

This study was conducted with the aim of attaining elastic softening of the three pure alkali cyanides of NaCN, KCN and RbCN using ETSM at very low temperature range which is different from the temperature ranges of our earlier studies [15]. Detailed investigation of the cohesive and thermal properties of these materials were carried out at very low temperatures with the frame work of ETSM. The cohesive energy [16], molecular force constant, compressibility, Debye temperature (θ_D) [17], Gruneisen parameter (γ) [18] and the ratio of volume expansion coefficient

(α_v) to volume specific heat (c_v) were calculated for all three pure Alkali Cyanides. Since there is a large size difference between M^+ (alkali) and CN^- ions in Alkali Cyanides, this potential model is effective in explaining them. As the Cauchy discrepancy in these crystals are much larger than that of alkali halides the effect of three body interaction will be much significant in them.

The temperature dependent second order elastic constants which included translation – rotational coupling effect have been calculated using the potential model of ETSM. The modified equations for second order elastic constants of NaCl structure with temperature dependence are given as,

$$\boldsymbol{C_{11}(T) = C_{11}^{0} - \frac{8}{r}A_{eff}^{2}\chi_{11}(T)} \quad \textbf{(3a)}$$

$$\boldsymbol{C_{12}(T) = C_{12}^{0} + \frac{4}{r}A_{eff}^{2}\chi_{11}(T)} \quad \textbf{(3b)}$$

$$\boldsymbol{C_{44}(T) = C_{44}^{0} - \frac{2}{r}A_{eff}^{2}\chi_{44}(T)} \quad \textbf{(3c)}$$

The temperature dependent rotational susceptibility (χ_{11}, χ_{44}) is calculated from the theory of Sahu and Mahanti [19]. The temperature dependence of c_{11}, c_{12} and c_{44} arises from the short – range repulsion and also from the contributions of quadrupole to the translational – rotational coupling. The bare elastic constants, c^o_{11}, c^o_{12}, and c^o_{44} depend on the rotational susceptibility [10]. The three parameters in ETSM are hardness parameter b, range parameter ρ and TBI parameters f(r). The hardness and range parameters are determined from the equilibrium condition,

$$\boldsymbol{\left|\frac{d(r)}{dr}\right|_{r=r_0} = 0} \quad \textbf{(4)}$$

and the equation,

$$\boldsymbol{B = (9K_{r_0})^{-1}\left|\frac{d^2(r)}{dr^2}\right|_{r-r_0}} \quad \textbf{(5)}$$

The function $f(r)$ is the long range TBI parameter and its higher order derivatives are obtained by the expression [20],

$$\boldsymbol{f(r) = f_0 e^{-r/\rho}} \quad \textbf{(6)}$$

The interionic separation at different temperature is obtained by the linear expression.

$$\boldsymbol{r = r_0(1 + \alpha T)} \quad \textbf{(7)}$$

Where, r_o represents the equilibrium interionic distance and α represents the linear thermal expansion coefficient [21] and the temperature is expressed as T.

The cohesion in a crystal system can be expressed as the cohesive energy (Φ) of a material. If the cohesion for the material is negative it means that the constituent atoms will gain energy by reacting to form a compound (solid or molecule). The calculation of cohesive energy from the interatomic potentials will give a clear idea about the binding energy of ionic crystals. Tosi Sangster et al [16] have given the details of these potentials .The expression for cohesive energy of alkali cyanides is given in equation 1.

The compressibility is given by,

$$\boldsymbol{\beta} = \frac{3K_{r_0}}{f} \tag{8}$$

Where, r is the interatomic separation, K is the crystal structure constant and f is the molecular force constant which is given as,

$$\boldsymbol{f} = \frac{1}{3}\left[\Phi_{kk'}^{SR}(\boldsymbol{r}) + \frac{2}{r}\Phi'^{SR}_{kk'}(\boldsymbol{r})\right] \tag{9}$$

Here, the short – range nearest neighbour (k = k ') part of Φ (r) is expressed as $\Phi_{kk'}^{SR}(r)$which is obtained from the last three terms in eqn 1.The Restrahlen frequency can be expressed as,

$$\boldsymbol{\vartheta_0} = \frac{f/\mu^{1/2}}{2\pi} \tag{10}$$

Where, μ represents the reduced mass of the alkali cyanides. The equation for Debye temperature is,

$$\boldsymbol{\theta_D} = \frac{h\vartheta_0}{K_B} \tag{11}$$

Where, K_B and h are the Boltzmann's constant and Planck's constant respectively. The expression for Gruneisen parameter is,

$$\boldsymbol{\gamma} = \frac{r_0}{6}\left|\frac{\phi'''(r)}{\phi''(r)}\right|_{r=r_0} \tag{12}$$

Where, the interatomic separation is expressed as $\boldsymbol{r_0}$ and the third and second order derivatives of potential energy are given as $\phi'''(r)$ and $\phi''(r)$ are respectively.

The expression [4] for ratio of volume expansion coefficient to volume specific heat is given as,

$$\frac{\alpha_v}{C_v} = -\left|\frac{\phi'''(r)}{2r\phi''(r)}\right|_{r=r_0} \tag{13}$$

3. RESULTS AND DISCUSSION

The potential model of ESTM has been used to compute the temperature dependent second order elastic constants (SOECs) of alkali cyanides [10, 22] such as NaCN, KCN and RbCN. The values of input data corresponding to NaCN, KCN and RbCN have been tabulated in table1. Here r_o is the equilibrium interionic distance [23], c_{11}, c_{12}, c_{44} are elastic constants [18], υ_{TO} is zone centre vibration frequency [24, 25] α_+ and α_- the electronic polarizabilities and ε_0 and ε_α are the dielectric constants [26, 27]. The values of van der Waals coefficients of NaCN, KCN and RbCN are given in table 2 which is considered for determining the model parameters.

The model parameters were computed at different temperature for NaCN, KCN and RbCN using the equations 3-5 with the data given in table 1 and are listed in table 3(a), 3(b) and 3(c) respectively.

The SOECs in the temperature range of 172K≤ T ≤552K for NaCN, 115K≤ T≤455K for KCN and 164K≤ T ≤ 544K for RbCN were calculated using the equation 3 and the model parameters. The exact effect of TR coupling is revealed as the calculations have been performed with and without TR. The variation of the second order elastic constants of NaCN, KCN and RbCN with temperature are represented graphically in figures 1 to 9. The temperature dependence of SOEC's were calculated with TR [$C_{ij}(T)$] and without TR [C_{ij}(without)] and the experimental data [C_{ij}(expt)] for NaCN is shown in those figures.

The calculated values of SOEC's such as c_{11}, c_{12} and c_{44} without TR called as the bare elastic constants are not in agreement with the experimental results. The SOEC's c_{11}, c_{12} and c_{44} calculated with the inclusion of TR coupling which are given as c_{11} (T), c_{12} (T) and c_{44} (T) are compared with the experimental data [7, 28-30]. The graphical observations indicate that there is an increase in c_{11} and c_{44} with increase in temperature for alkali cyanides. This might be due to the crucial role played by the temperature in c_{11} and c_{44}. The existence of reduction at the lower temperature range is indicated by the increasing trends of c_{11} and c_{44}.The anomalous softening of shear elastic constant c_{44} is an important feature of the phase transition of alkali cyanides. c_{12} decreases with increase in temperature and shows quasilinear behaviour similar to the experimental results. Thus, a fairly good agreement between the theoretical and experimental results is shown with the inclusion of TR coupling effects.

Using the above equations from 1 and 8-13, the cohesive and thermal properties of NaCN, KCN and RbCN were computed and tabulated in tables 4 (a), (b) and (c) respectively. The results given in table 4 shows that the cohesive energy, the Restrahlen frequency and the molecular force constant show decreasing pattern with increasing temperature. Whereas, there is an increasing trend for the compressibility with the increase in temperature. The results follow the similar trend for the three alkali cyanides, NaCN, KCN and RbCN. The results in comparison with experimental results at room temperature [31-34] were found to be in closer agreement. The stability of the compound is indicated through the negative values of cohesive energy. The repulsive part is almost 10% of the total cohesive energy which indicates that the cohesion in ODM might be mainly due to the Columbic contribution. Also, the Debye temperature is decreasing slightly with the increasing temperature. The Debye temperatures obtained from this study is found to be more accurate since the elastic constants which are temperature dependent have been considered. The lower phonon frequencies in these materials are indicated through the lower values of Debye temperature. The temperature dependence of θ_D is useful for understanding the thermodynamic behaviour of solids. The Grunesien parameter shows an increasing trend with temperature whose values appear more realistic and show high degree of agreement with the measured values for Alkali – Halides. The values of $\frac{\alpha_v}{C_v}$ also increase with increase in temperature for all the three alkali cyanides.

4. CONCLUSION

The results conclude that the elastic constants in ODMs are softened by the translational – rotational coupling effect at the zone center. The shear elastic constants are found to indicate softening at the lower temperature side which might be due to the effective coupling of CN^- ion. The decreasing of c_{44} at transition temperature in NaCN, KCN and RbCN reveals the geometrical situation of the cyanide ions in the octahedral cage of cations. The barrier for the hindered vibrational and rotational motion of the CN^- ion is weakened in this sequence as the lattice constant and the voids within the octahedral cage increases with the atomic number of the monovalent cations under investigation. So the thermal energies required to induce their motion is lowered.

The TR coupling effect is found to be important in assessing the dependence on temperature of the second order elastic constants. In addition, the temperature dependence of c_{44} shows the collective behavior of the coupled impurity. Hence, it can be concluded that the potential model, ETSM is an appropriate model which explains the important physical properties of orientationally disordered pure alkali cyanides at various temperatures. The calculated results show an excellent agreement with experimentally obtained results. This reveals that ETSM is an adequately suitable model for the unified and comprehensive study of orientationally disordered materials. Even though some results presented are only of academic nature, they can still guide the experimental works in future.

REFERENCES

[1]W.C. Overtone Jr. and R.T.Swim, *PhysRev*.**84**, 758 (1951)

[2]M.H. Norwood and C.V.Briscoe, *Phys.Rev*.**112**, 45 (1958)

[3]R.K. Singh, *Phys.reports* **85**, 259 (1982)

[4]R.K.Singh and N.K.Gaur, *Physica* **B+ C , 150**, 385 (1988)

[5] Shemim S S, Rasna Thakur, N.K. Gaur, *Advances in Physics Theories and Applications* ISSN 2224-719X, **Vol.45**, 2015

[6]D.W.Hafemeister and W.H. Flygare, *J.Chem. Phys*,**43**, 795 (1965)

[7]K.H.Michel and J.Naudts *, J.Chem. Phys.***67**,547 (1977)

[8]D.Sahu and S.D. Mahanti, *Phys.Rev.*B **26**, 2981 (1982)

[9]F. Luty in "*Defects in Insulating Crystals"* ed. V.M. Turkevich and K.K. Shvarts (Springer Verlarg, Berlin, 1981) p 69.

[10] Preeti singh, NK Gaur, RK Singh Physica, status solidi (b), Vol 244, 09/2007

[11] A.R. Verma, O.N. Shrivastava, *"Crystallography for Solid State Physics",* (Willey Eastern, New Delhi, 1983)

[12] Shemim S S, N.K. Gaur, "*Imperial Journal of Interdisciplinary Research* "2 (11), 2016 ISSN: 2454-1362

[13]K.H.Michel and J.Naudts, *Phys.Rev.Lett*.**39**, 212 (1977)

[14]R.Narayan, *J. Phys.Chem.solids*.**38**,1097 (1977)

[15]Preethi Singh and N.K Gaur, Phys.Lett.**A371**, 349 (2007).

[16]M.J.L. Sangster, *J. Phys. Chem. Solids* **34**, 335 (1973)

[17]H. Siethoff and K. Ahlborn, *Phys. State Sol.* (b) **190**, 179 (1995)

[18]J. Shanker, K Singh, *Phys. State Sol.* (b) **109**, 411 (1982)

[19]D. Sahu and S.D. Mahanti*, Solid State Commun*. **47**, 207 (1983)

[20]P.O. Lowdin, Ark. Fys. **35A,** 30 (1947)

[21]S.Haussuhl, Acta. Cryst**. A30**, 455 (1974)

[22] S.Haussuhl ,*Solid State Commun*. **13**, 147 (1973)

[23] C.Kittel, "*Introduction to Solid State Physics*" 5th Ed. (Wiley Eastern, New Delhi, 1988)

[24]J.M. Rowe, J.J. Rush, N.Vegelators, D.L. Price D.G. Hinks and S.Suman, *J. Chem. Phys***. 62,** 4551 (1975)

[25]J.M. Rowe, J.J. Rush, E Prince and J.J. Chesser*, Ferroelectrics* **16** 107 (1977)

[26]K.D. Ehrhardt, W.Press, J.Lefebvrae, S.Haussuhl, *Solid State Commun*. **34**, 580 (1980)

[27]J.R. Tessmann, A.H. Khan, W. Schockley*, Phys. Rev*. **B92**, 890 (1953)

[28]S. Haussuhl, J. Eckstein, K. Recker and F. Wallrafen, *Acta. Cryst***. A 33,** 847 (1977)

[29]S. Haussuhl, Z. Kristallogr. 110, 67 (1958)

[30]J.O.Fossum, A. Wells and Garland, *Phys.Rev*.**B38,** 412 (1988)

[31]R.C. Weast (ed) "*CRC Handbook of Physics and Chemistry"* (CRC Press 1981) D89

[32]David R Lied (ed) "*CRC Handbook of Physics and Chemistry"* 76th addition CRC Press 12-21-39(1995-1996)

[33].M.L.Klein,Y.Ozaki and I.R.Mc Donald, J.*phys.Chem* **15**,4993 (1982).

[34]L.Vegard, *Z.Phys*,**5**, 17 (1921).

Table 1**.** Input data for pure alkali cyanides.

Properties	**NaCN**	**KCN**	**RbCN**
$r_0(A^o)$	2.94	3.26	3.42
c_{11} (10^{11}dynes/cm^2)	2.53	1.91	1.75
c_{12} (10^{11}dynes/cm^2)	1.44	1.19	1.04
c_{44} (10^{11}dynes/cm^2)	0.03	0.14	0.17
$_{TO}$ (THZ)	4.3	4.11	4.23
$\alpha_+ (A^o)^3$	0.28	1.3	2.1
$\alpha_- (A^o)^3$	1.8	1.8	1.8
ε_0	7.55	5.72	4.5
ε_α	2.1	1.99	1.77

Table 2 Van der Waals co-efficient for pure alkali cyanides crystals ($c_{kk'}$ and $d_{kk'}$ are in the units of 10^{-60} erg .cm^6, 10^{-76} erg. cm^8 respectively)

Compound	**C**	**D**	$\mathbf{c_{kk'}}$	$\mathbf{c_{kk}}$	$\mathbf{c_{k'k'}}$	$\mathbf{d_{k'k'}}$	$\mathbf{d_{kk}}$	$\mathbf{d_{k'k'}}$
NaCN	251.19	89.52	20.86	5.89	105.25	10.46	1.49	61.56
KCN	678.41	277.49	79.79	63.22	102.25	39.56	24.26	61.56
RbCN	1164.5	502.86	137.28	181.6	105.25	72.36	83.76	61.56

Table 3 (a). Model parameters for NaCN in the range 172 K $\leq T \leq$ 552 K

T(K)	**r(A^o)**	**ρ(A^o)**	**b(10^{-12} ergs)**	**f(r)**
172	2.9914	0.3623	0.6612	-0.025
192	3.0057	0.3627	0.6652	-0.025
212	3.0089	0.3631	0.6699	-0.0251
232	3.0097	0.3633	0.6728	-0.0251
252	3.0138	0.3637	0.6771	-0.0251
272	3.0169	0.3641	0.6801	-0.0252
292	3.0192	0.3647	0.6851	-0.0252
312	3.023	0.365	0.6885	-0.0252
332	3.0251	0.3654	0.6913	-0.0253
352	3.0268	0.3657	0.6962	-0.0253
372	3.0291	0.3658	0.6994	-0.0253
392	3.0328	0.3661	0.703	-0.0254
412	3.0358	0.3663	0.7068	-0.0254
432	3.0388	0.3665	0.7097	-0.0254

452	3.0419	0.3667	0.7139	-0.0255
472	3.0448	0.3669	0.7182	-0.0255
492	3.0473	0.3671	0.7208	-0.0256
512	3.0512	0.3673	0.7234	-0.0256
532	3.0548	0.3675	0.7268	-0.0256
552	3.0576	0.3677	0.7291	-0.0256

Table(3(b). Model parameters for KCN in temperature range 115 K $\leq$ T $\leq$ 455 K

T(K)	**r(A^o)**	**ρ(A^o)**	**b(10^{-12}** ergs)	**f(r)**
105	3.2339	0.3422	0.56843	-0.023
115	3.2359	0.34241	0.57112	-0.023
135	3.2399	0.34284	0.57621	-0.0231
155	3.2449	0.34353	0.58321	-0.0231
175	3.2489	0.34372	58634	-0.0231
195	3.2529	0.34291	0.5961	-0.0231
215	3.2568	0.3441	0.5998	-0.0232
235	3.2601	0.34433	0.60812	-0.0232
255	3.2647	0.34451	0.61091	-0.0232
275	3.2668	0.34474	0.61919	-0.0232
295	3.271	3.34493	0.62513	-0.0233
315	3.2724	0.34513	0.63212	-0.0233
335	3.2725	0.34534	0.63744	-0.0233
355	3.2727	0.34556	0.64231	-0.0234

375	3.2731	0.34572	0.64822	-0.0234
395	3.2751	0.34591	0.65513	-0.0235
415	3.2772	0.34623	0.65911	-0.0235
435	3.2793	0.34642	0.66412	-0.0236
455	3.281	0.34661	0.66714	-0.0236

Table 3(c). Model parameters for RbCN in temperature range 164 K $\leq$T$\leq$ 544K.

T(K)	**r(A^o)**	**ρ(A^o)**	**b(10^{-12} ergs)**	**f(r)**
164	3.383	0.3524	3.489	-0.02297
184	3.387	0.3528	3.499	-0.02297
204	3.391	0.3532	3.509	-0.02298
224	3.395	0.3536	3.519	-0.02298
244	3.398	0.3539	3.528	-0.02299
264	3.402	0.3542	3.529	-0.02299
284	3.406	0.3546	3.549	-0.02299
304	3.41	0.3549	3.56	-0.023
324	3.414	0.3553	3.57	-0.023
344	3.418	0.3557	3.579	-0.023
364	3.422	0.3561	3.589	-0.02301

384	3.426	0.3565	3.599	-0.02301
404	3.43	0.3568	3.609	-0.02301
424	3.434	0.3572	3.619	-0.02302
444	3.438	0.3576	3.629	-0.02302
464	3.446	0.358	3.639	-0.02302
484	3.446	0.3584	3.649	-0.02303
504	3.45	0.3587	3.658	-0.02303
524	3.454	0.359	3.667	-0.02303
544	3.458	0.3594	3.677	-0.02304

Table 4 (a) Thermal properties of NaCN in temperature range 172K≤ T≤ 552 K.

T (K)	ϕ (KJ mol^{-1})	B (10^{-12} dyne/cm^2)	F (10^4dyne/cm)	υ_0 (THz)	θ_D (K)	α_v/c_v (10^3J)	Γ
172	-758.26	5.058	1.928	3.998	180.78	4.402	1.562
192	-756.46	5.086	1.924	3.979	180.52	4.418	1.562
212	-753.68	5.099	1.908	3.958	180.24	4.434	1.563
232	-750.69	5.127	1.893	3.937	179.93	4.455	1.564
252	-746.83	5.153	1.877	3.919	179.68	4.473	1.566
272	-743.74	5.182	1.862	3.9	179.37	4.492	1.566
292	-739.16	5.21	1.846	3..882	178.98	4.511	1.567
312	-735.56	5.238	1.831	3.862	178.58	4.528	1.568
332	-731.82	5.256	1.815	3.841	178.29	4.551	1.569
352	-728.73	5.284	1.8	3.822	177.81	4.581	1.57

372	-724.84	5.312	1.784	3.802	177.48	4.614	1.571
392	-720.59	5.34	1.768	3.782	177.2	4.634	1.572
412	-716.42	5.368	1.752	3.762	176.8	4.651	1.573
432	-712.32	5.396	1.737	3.741	176.43	4.673	1.574
452	-708.87	5.424	1.723	3.72	176.19	4.698	1.575
472	-704.26	5.452	1.708	3.702	175.88	4.718	1.576
492	-700.13	5.477	1.691	3.681	175.51	4.741	1.577
512	-696.45	5.512	1.679	3.664	175.25	4.764	1.578
532	-692.87	5.537	1.664	3.643	174.89	4.782	1.579
552	-688.37	5.555	1.653	3.622	174.53	4.812	1.58
Expt	-738	5.56	3.18	-	-	-	-

Table 4 (b) Thermal properties of KCN in temperature range 115K ≤ T≤ 455 K.

T (K)	ϕ (KJ mol^{-1})	B (10^{-12} dyne/cm^2)	F (10^4dyne/cm)	υ_0 (THz)	θ_D (K)	α_v/c_v (10^3J)	Γ
115	-695.21	6.071	4.508	3.489	186.14	8.789	1.643
135	-694.32	6.078	4.463	3.463	185.93	8.814	1.644
155	-693.62	6.086	4.426	3.452	185.74	8.821	1.645
175	-692.97	6.091	4.389	3.447	185.51	8.834	1.545
195	-692.23	6.097	4.341	3.442	185.23	8.842	1.646
215	-691.57	6.124	4.302	3.432	184.77	8.847	1.647
235	-690.97	6.132	4.269	3.426	184.38	8.854	1.648
255	-690.38	6.193	4.221	3.419	183.74	8.862	1.649
275	-689.68	6.204	4.096	3.415	183.21	8.865	1.651
295	-688.83	6.225	4.055	3.407	182.83	8.872	1.653

315	-687.89	6.274	4.018	3.398	182.48	8.88	1.655
335	-687.12	6.438	3.086	3.392	182.13	8.892	1.657
355	-686.28	6.518	3.027	3.385	181.68	8.904	1.659
375	-685.85	6.553	3.001	3.377	181.25	8.913	1.661
395	-685.48	6.593	2.981	3.369	180.81	8.926	1.663
415	-685.04	6.641	2.958	3.361	180.65	8.933	1.665
435	-684.61	6.684	2.934	3.353	180.48	8.947	1.668
455	-685.24	6.721	2.911	3.345	180.23	8.961	1.67
Expt	-674	6.95	2.82	4.11	197	-	-

Table 4 (c) Thermal and Cohesive properties of RbCN in the temperature range 164 K≤ T ≤ 544K

T (K)	ϕ (KJ mol^{-1})	β (10^{-12} dyne/cm^2)	F (10^4dyne/cm)	υ_0 (THz)	θ_D (K)	α_v/c_v (10^3J)	Γ
164	-648.32	6.657	2.529	4.2604	220.78	5.272	1.743
184	-647.91	6.673	2.526	4.2601	220.63	5.277	1.746
204	-647.58	6.695	2.522	4.2597	220.48	5.282	1.749
224	-647.12	6.71	2.519	4.2594	220.32	5.286	1.751
244	-646.76	6.722	2.515	4.259	220.16	5.291	1.755
264	-646.33	6.737	2.512	4.2587	220.02	5.295	1.757
284	-645.97	6.753	2.508	4.2583	219.95	5.299	1.76
304	-645.56	6.769	2.504	4.258	219.8	5.302	1.763
324	-645.12	6.785	2.501	4.2576	219.65	5.306	1.766
344	-644.75	6.801	2.497	4.2572	219.5	5.309	1.769
364	-644.34	6.82	2.493	4.2569	219.55	5.311	1.772
384	-643.98	6.837	2.489	4.2565	219.39	5.316	1.775

404	-643.57	6.853	2.486	4.2561	219.24	5.32	1.778
424	-643.14	6.869	2.482	4.2558	219.08	5.323	1.782
444	-642.75	6.885	2.478	4.2554	218.93	5.326	1.786
464	-642.34	6.904	2.474	4.2549	218.77	5.329	1.79
484	-641.92	6.913	2.47	4.2545	218.61	5.331	1.794
504	-641.55	6.933	2.466	4.2541	218.44	5.334	1.798
524	-641.13	6.948	2.462	4.2536	218.27	5.337	1.802
544	-640.76	6.964	2.458	4.2531	218.12	5.341	1.806
300	-646	7.83	2.62	4.23	203	-	-

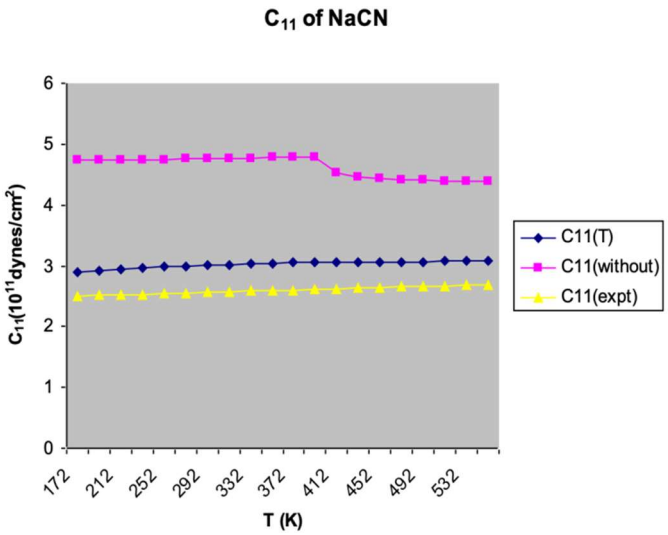

Fig.1: C_{11} of NaCN

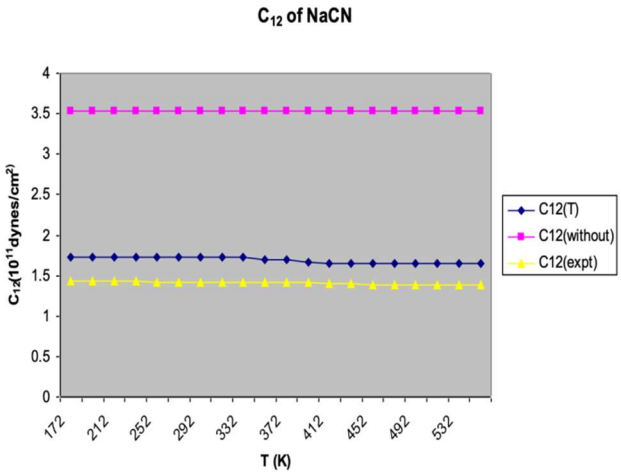

Fig.2: C_{12} of NaCN

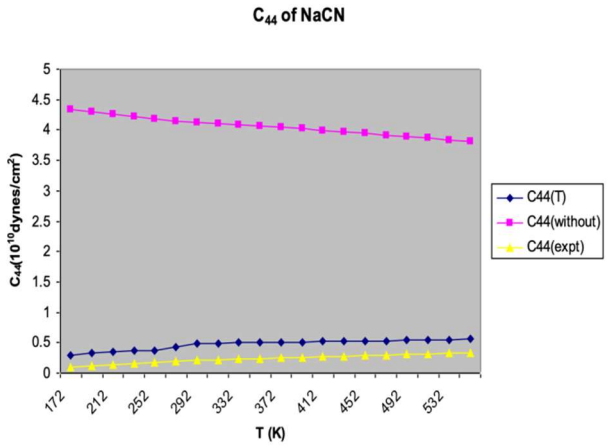

Fig.3:C_{44} of NaCN

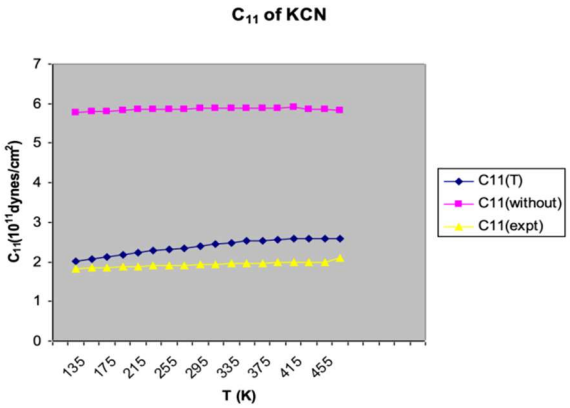

Fig.4: C_{11} of KCN

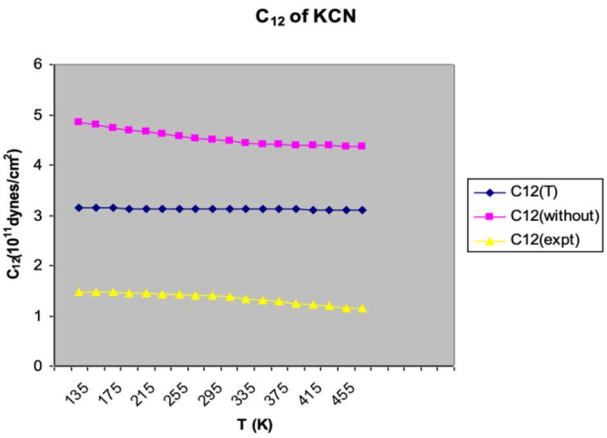

Fig.5:C_{12} of KCN

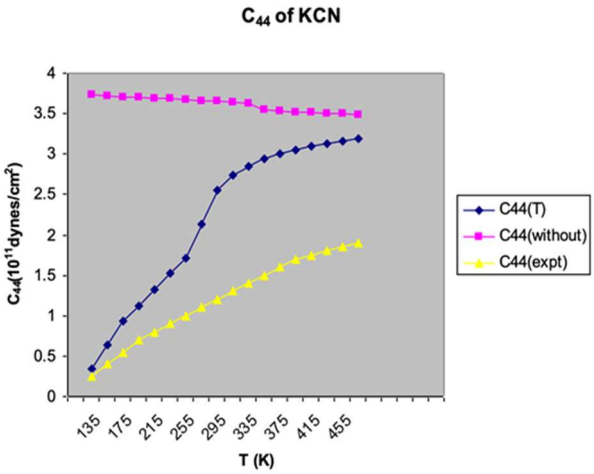

Fig.6: C_{44} of KCN

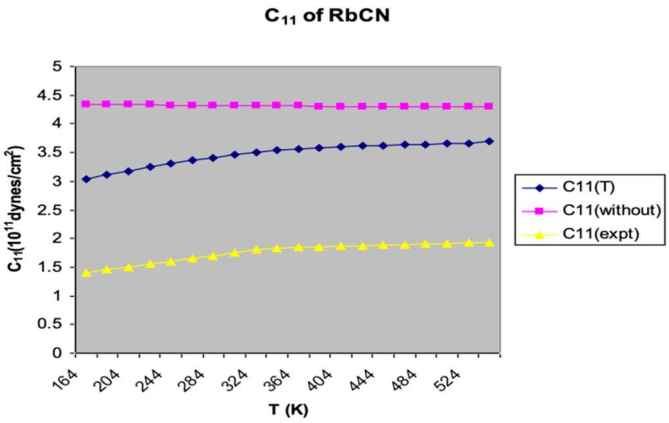

Fig.7:C_{11} of RbCN

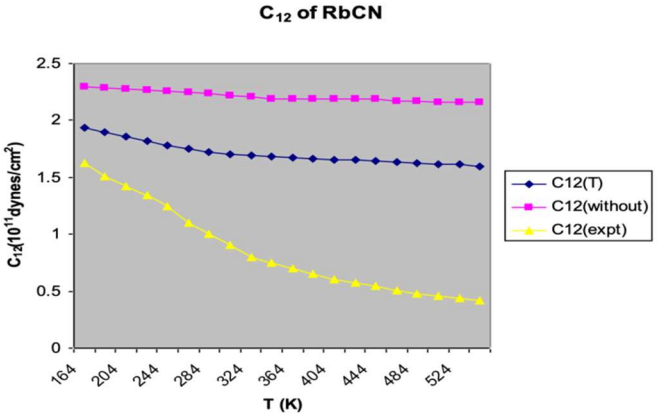

Fig.8:C_{12} of RbCN

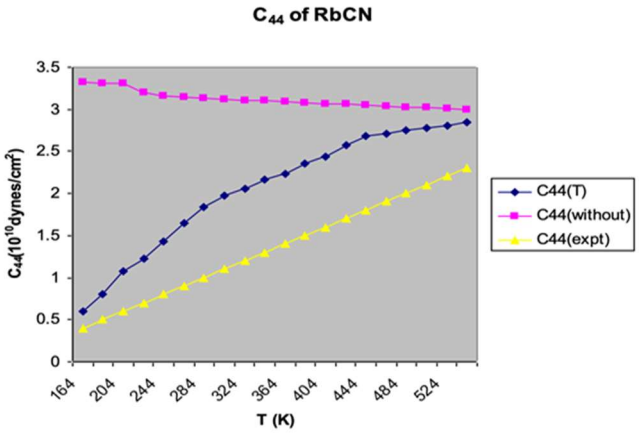

Fig.9:C_{44} of RbCN